Effects of chemical and green nano-zinc oxide on histological changes, oxidative stress, and apoptosis in rat kidney associated with cisplatin

Naeem Erfani Majd[1, 2], Mohammad Reza Tabandeh[2,3]*,
Shima Hosseinifar[1], Anahita Rezaie[4], Hajar Papi[1]

[1]Department of Basic Sciences, Histology Section, Faculty of Veterinary Medicine, Shahid Chamran University of Ahvaz, Ahvaz, Iran, [2]Stem Cell and Transgenic Technology Research Center of Shahid Chamran University of Ahvaz, Ahvaz, Iran, [3]Department of Basic Sciences, Division of Biochemistry and Molecular Biology, Faculty of Veterinary Medicine, Shahid Chamran University of Ahvaz, Ahvaz, Iran, [4]Department of Pathobiology, Faculty of Veterinary Medicine, Shahid Chamran University of Ahvaz, Ahvaz, Iran

Cisplatin (CP) is used to treat various tumors. A main restriction of cisplatin is nephrotoxicity. This study aimed to evaluate the protective effects of ZnONPs on cisplatin-induced oxidative stress and rat kidney tissue damage. Eighty adult male Wistar rats (250g-270g) were divided into ten groups: Control (CON), Sham (SH), Bulk ZnO (BZnO), Chemical ZnONPs (ChZnONPs), Green ZnONPs (GrZnONPs), Cisplatin (CP), Cisplatin+BulkZnO (CP+BZnO), Cisplatin+Green ZnONPs (CP+GrZnONPs), Cisplatin+Chemical ZnONPs (CP+ChZnONPs), Cisplatin+Explant (CP+EX). CP was i.p administered 5mg/kg/week and BZnO, ChZnONPs and GrZnONPs were i.p administered at a dose of 5mg/kg/day. After 30 days of the treatment, the expression of apoptosis/anti apoptosis related genes oxidant/antioxidant factors and histological changes in the were studied. The CP-treated group showed a decrease in body weight, while the Co-administration of ZGNPs to CP-treated rats showed a significant increase compared to the CP group. The results showed that the increased mRNA level of bax, MDA and the decreased mRNA level of bcl2, SOD and CAT activities in kidney of CP group were improved when animals were treated with ZnO NPs. Our results showed that GrZnONPs, ChZnONPs and BZnO had the potential to protect against oxidative stress and cisplatin-induced neurotoxicity that this protective effect was more evident in GrZnONPs.

Keywords: Cisplatin. Zinc Oxide Nanoparticles. Kidney. Histology. Apoptosis.

INTRUDUCTION

Cisplatin (CP) is a chemotherapeutic drug used in cancer treatment, however, numerous side effects and toxicities limit the use of CP. Nephrotoxicity has been recognized as one of the most serious complications associated with CP (Akca *et al.*, 2018). The kidney collects CP more than other sections in the body and is the main pathway for its disposal. CP accumulates more in the S3 section of the proximal tubules, followed by the distal tubules, and S1 section of the proximal tubules (Kröning, Lichtenstein, Nagami, 2000; Yao *et al.*, 2007). Nephrotoxicity of cisplatin is evident by decreasing antioxidant enzyme activity, a concomitant decrease in glutathione levels, increased lipid membrane peroxidation, and mitochondrial dysfunction (Akca *et al.*, 2018; Zhang *et al.*, 2019). Also, nephrotoxicity causes direct tubular damage, vascular abnormalities, oxidative stress, inflammation, fibrogenesis, apoptosis and necrosis. It has been confirmed that cisplatin with high reactive oxygen species (ROS) production causes an imbalance between the level of oxidant-antioxidant factors, thus the level of antioxidants to neutralize

produced ROS is undesirable in tissue (Akca *et al.*, 2018). The nephrotoxicity of CP is now detected as a very complex process (Pabla, Dong, 2008).

CP induced nephrotoxicity leads to the changes in the apoptosis-related proteins. It has been reported that nephrotoxicity of CP causes increase in the *bax* (pro-apoptotic protein) and a decrease in the *bcl-2* (anti-apoptotic protein expression) (Tsuruya *et al.*, 2003). The route involvement of the apoptosis in the CP-induced kidney injury was at first suggested with *bax* accumulation in the mitochondria and cytochrome c release in cultured kidney cells (Pabla, Dong, 2008).

Zinc as an antioxidant has an important protective role against oxidative stress (Roy *et al.*, 2013; Rabeea *et al.*, 2016). ZnO NPs is used because of its properties such as abundance, semi-conductivity, non-toxic effect and bond strength and many more. ZnO NPs are the most prominent because of their low cost production, suitability for use in food preservation, and their effectiveness to promote immunity (Hamza, Al-Salmi, El-Shenawy, 2019). ZnO NPs are synthesized by (i) physical, (ii) chemical, and (iii) green or biogenic methods. The green or biogenic ZnO NPs can be produced from plants, algae, fungi, and bacteria which results in much less use of chemicals, less pollution, less cost and less energy (Sharmila, Thirumarimurugan, Muthukumaran, 2019). Among these, plant synthesis has attracted more attention due to their high availability, greater sustainability, faster synthesis rate, non-hazardous, cost-effective and simple methods (Iravani, 2011; Jeevanandam, Chan, Danquah, 2016; Khan, *et al.*, 2018).

Based on our knowledge the comparative protective effect of chemical and green synthesized ZnO NPs against CP toxicity has not been reported in the rat's kidney. This study was designed to examine the possible protective effect of GrZnO NPs in comparison to ChZnO NPs and BZnO NPs on kidney tissue following cisplatin chemotherapy. The antioxidant and antiapoptotic properties of different forms of ZnO, as possible protective mechanisms against CP induced nephrotoxicity were also studied.

MATERIAL AND METHODS

Synthesis of nanoparticles

Plant collection

The Fresh green leaves of *Aleo vera* were collected from September to January (Santhoshkumar, Kumar, Rajeshkumar, 2017).

preparation of the plant extract

Five g of *Aleo vera* leaves were freshly washed and crushed, then mixed with 100 ml of distilled water, warmed to 70 ° C for 8 min and filtered using filter paper (Santhoshkumar, Kumar, Rajeshkumar, 2017).

Green ZnO NPs preparation and characterization

GrZnO NPs synthesis was performed using *Aloe vera* leaf extract as described previously (Santhoshkumar, Kumar, Rajeshkumar, 2017). Briefly, Zinc acetate dehydrate (Merck-Germany) (50 ml of 1 mM) was kept in stirrer for 1h, followed by dropwise addition of NaOH solution (25 mL of 5mM). The stirring of the mixed solution was continued for about 30 min and then the plant aqueous extract (Local store -Urmia) (%10 w/w) was added to the reaction. The reaction was continuously stirred and heated to 65 for another 30 min. The color change of the solution and the appearance of yellow slurry approved the formation of ZnO NPs. After the samples were centrifuged at 8000 × rpm for 10 min, the supernatant was decanted and the participant was washed extensively with ethanol and deionized water to remove the unreacted reagents. Finally, the obtained solid materials were finally dried under vacuum condition at 80 for 2hr. The size and morphology of the prepared ZnO NPs were assessed using TEM (Leo 906 E. Carl Zeiss. Germany) and PSA (Scatteroscope. Qudix Inc., South Korea).

Animals and experimental design

Eighty healthy adult male Wistar rats (250g - 270g) were retained under standard laboratory conditions of humidity, temperature (22 ± 2°C), and 12h light/dark

cycle (light from 7:00 to 19:00), with ad libitum access to food and tap water. After one week of acclimatization, the experimental animals were randomly divided into ten groups (n=8 per group) as follows. All the experimental protocols were approved by the ethics committee for research in animals and humans of Shahid Chamran University of Ahvaz (EE/98.24.3.26317/SCU.AC.IR). The animals were used according to the guidelines for the care and use of laboratory animals provided by the national academy of sciences (National Institutes of Health publication No. 86-23).

Group 1: Control group (CON): rats were received 2 ml/kg saline (i. p).

Group 2: Sham group (SH): rats were maintained without any injections, fed normal feed, and in the same environmental conditions as the other groups.

Group 3: Bulk ZnO Group (BZnO): rats were administered 5 mg/kg BZnO daily for 4 weeks (i. p) (Torabi *et al*., 2013).

Group 4: Green ZnO NPs Group (GrZnO NPs): rats were administered 5 mg/kg GrZnO NPs daily for 4 weeks (i. p) (Torabi *et al*., 2013).

Group 5: Chemical ZnO NPs Group (ChZnO NPs): rats were administered 5 mg/kg ChZnO NPs daily for 4 weeks (i. p) (Torabi *et al*., 2013).

Group 6: Cisplatin group (CP): rats were administered 5 mg/kg CP once a week for 4 weeks (i. p) (Kiyani *et al*., 2019).

Group 7: Cisplatin + Bulk ZnO Group (CP + BZnO): rats were administered 5 mg/kg CP (i. p) once a week for 4 weeks and 5 mg/kg BZnO daily for 4 weeks.

Group 8: Cisplatin + Green ZnO NPs Group (CP + GrZnO NPs): rats were administered 5 mg/kg CP (i. p) once a week for 4 weeks and 5 mg/kg GrZnO NPs daily for 4 weeks (Torabi *et al*., 2013).

Group 9: Cisplatin + Chemical ZnO NPs Group (CP + ChZnO NPs): The rats were administered 5 mg/kg CP (i. p) once a week for 4 weeks and 5 mg/kg ChZnO NPs daily for 4 weeks (Torabi *et al*., 2013).

Group 10: Cisplatin + Explant Group (CP + EX): The rats were administered 5 mg/kg CP once a week for 4 weeks and *Aleo vera* extract (5 mg/kg/daily), for 4 weeks (i. p) (Torabi *et al*., 2013).

Serum Blood Urea Nitrogen assays

After overnight fasting, the rats were anesthetized using ketamine 100 mg/kg and xylazine 10 mg/kg. Heart blood samples were collected, and sera were separated and stored at -20°C for future use. Blood samples were centrifuged at 5000 × g for 5 min and sera were separated. Blood Urea Nitrogen (BUN) was determined spectrophotometrically using commertial kit as recommended by the manufacturer (ParsAzma, Iran).

Determination of Oxidative Stress Parameters

Briefly, a tissue specimen of 100 mg was homogenized in 1000 µl RIPA lysis buffer (NaCl; 150 mM, SDS 0.1%, Tris; 25 mM, pH 7.4, NaF; 1 mM, Phenylmethylsulfonyl fluoride 1 mM, Sodium Fluoride 50 mM) with a homogenizer (Heidolph, Germany). Homogenate was centrifuged at 10000 × RPM for 15 min at 4°C and supernatant was collected and stored at -20°C for subsequent analysis. Protein concentration was measured by bradford method and bovine serum albumin as standard.

The estimation of catalase and superoxide dismutase activities

Catalase activity was determined spectrophotometrically by the method of Koroliuk *et al*. (1988) Briefly, 10µL of sample was incubated with 100 µmol/mL of H_2O_2 in 0.05 mmol/L Tris-HCl buffer pH=7 for 10 min. The reaction was terminated by rapidly adding 50 µL of 4% ammonium molybdate. Yellow complex of ammonium molybdate and H_2O_2 was measured at 410 nm. One unit of catalase activity was defined as the

amount of enzyme required to decompose 1 μmol H2O2 per min. The activity of superoxide dismutase (SOD) was estimated using the commercial available kits (RANSOD, Randox Com, UK). The activities of antioxidant enzymes were expressed as IU/mg protein of tissue.

Measurement of lipid peroxidation

MDA was determined using the thiobarbituric acid reactive substance (TBARS) assay as described previously (Satoh *et al.*, 1978). Briefly, 100 uL of tissue homogenate was mixed thoroughly with 200 uL of 20% w/v trichloroacetic acid and 100 uL, 0.375% w/v thiobarbituric acid. The solution was sanded for 15 min in a boiling water bath. After cooling, the precipitate was removed by centrifugation at 5000 RPM for 10 min. The absorbance of the clear supernatant was determined at 532 nm. Quantification of the MDA level was determined at 532 nm by comparing the absorption to the standard curve of MDA equivalents generated by acid-catalyzed hydrolysis of 1,1,3,3-tetra methoxy propane. MDA results were expressed as nmol/mg protein of tissue.

RNA isolation and cDNA synthesis

Total RNA was isolated using RNX™ reagent according to the manufacturer's procedure (SinaClon, Iran). The concentration of extracted RNA was calculated at a wavelength of 260 nm using Eppendorf μ Cuvette G1.0 microvolume measuring cell (Eppendorf BioPhotometer D30, Eppendorf, Germany). To detect the purity of RNA, its optical density (OD) ratio at 260/280 nm was determined and samples with a ratio of >1.8

were used for cDNA synthesis. Reverse transcription was carried out using YTA cDNA synthesis kit and random hexamer primers as described by the manufacturer (Yektatajhiz, Iran).

Real-time quantitative real-time polymerase chain reaction

To evaluate the expression levels of *bax* and *bcl2* in the kidney, real-time PCR analysis was performed using qPCR™ Green Master Kit for SYBR Green I® (Yekta-Tajhiz, Iran) on a Lightcycler® Detection System (Roche, USA). Relative expression level of the Bax and Bcl2 transcripts were compared to rat GAPDH as the housekeeping gene. Specific sets of primers (Bioneer, South Korea) designed for this study are shown in table I. Reactions were performed using 12.5 μl mixtures containing 6.25 μl qPCR™ Green Master Kit for SYBR Green I® (YektaTajhiz, Iran), 0.25 μl of each primer (10 nM), 3 μl cDNA (100 ng), and 2.25 μl nuclease-free water. The PCR protocol consisted of a 5-min denaturation at 94°C followed by 45 cycles at 94ºC for 15 seconds, and at 60°C for 30 seconds. Reactions were performed in triplicate. Two separate reactions without cDNA or with RNA were performed in parallel as controls. Relative quantification was performed according to the comparative $2^{-\Delta\Delta Ct}$ method using Lightcycler 96® software. Validation of assay, in order to check that primer for target genes and GAPDH had similar amplification efficiencies, was performed as described previously. All qPCR analyses were performed according to The Minimum Information for Publication of Quantitative Real-Time PCR Experiments (MIQE) guideline.

TABLE I - List of primers used for Real-time PCR analysis

Gene name	Sequences	Size (bp)	GenBank
Bax	F: TGCTACAGGGTTTCATCCAG R: TGTTGTTGTCCAGTTCATCG	145	NM_017059.2
Bcl2	F:ATCGCTCTGTGGATGACTGAGTAC R:AGAGACAGCCAGGAGAAATCAAAC	135	NM_016993.1
GAPDH	F: AGTTCAACGGCACAGTCAAG R: TACTCAGCACCAGCATCACC	119	XM_017593963.1

Histological study

The tissue Kidney samples were fixed in 10% formalin buffer and 5-6 μm sections were made using paraffin embedding method. Hematoxylin-Eosin staining was used (Akca *et al*., 2018). Study was performed under light microscope using Dino Lite lens (Dino capture software, FDP2).

Statistical analysis

All data analyses were performed using the Statistical Package of Social Sciences (SPSS) software program, version 20 (SPSS; Chicago, IL, USA). One-way analysis of variance followed by the tukey test was used to test differences between various means. The data is presented as mean ± standard error of mean (SEM), and a P value of <0.05 was considered statistically significant.

RESULTS AND DISCUSSION

Characterization of GrZnO NPs

To confirm the morphological and physical properties of green synthesized ZnO NPs, an analysis of the samples was performed using (TEM) and particle size analyzer techniques. TEM micrograph clarified that ZnO NPs mostly exist in spherical shapes with 20-50 nm diameter (Figure 1A). The PSA graph which showed that the prepared NPs had narrow size distribution and >95% of ZnO were 10-65 nm in size and an average size about 36 nm (Figure 1B).
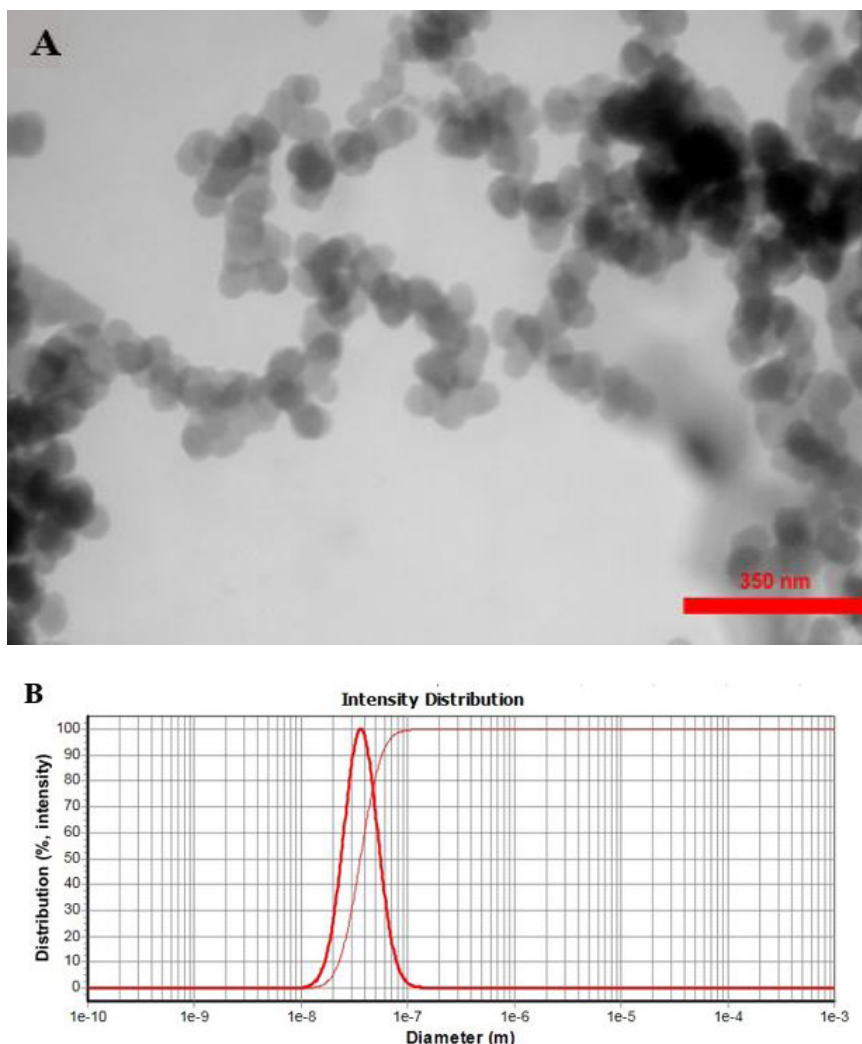

FIGURE 1 - TEM Images and Particle Size Analysis of green ZnO NPs.

Weight change in experimental groups

Rats' weight decreased significantly in the CP group compared to the control group (P < 0.05). A significant increase in body weight was observed only in the CP + GrZnO NPs compared to the CP groups (P <0.05). Treatment by other forms of ZnO had no obvious effect on body weight (Figure 2).
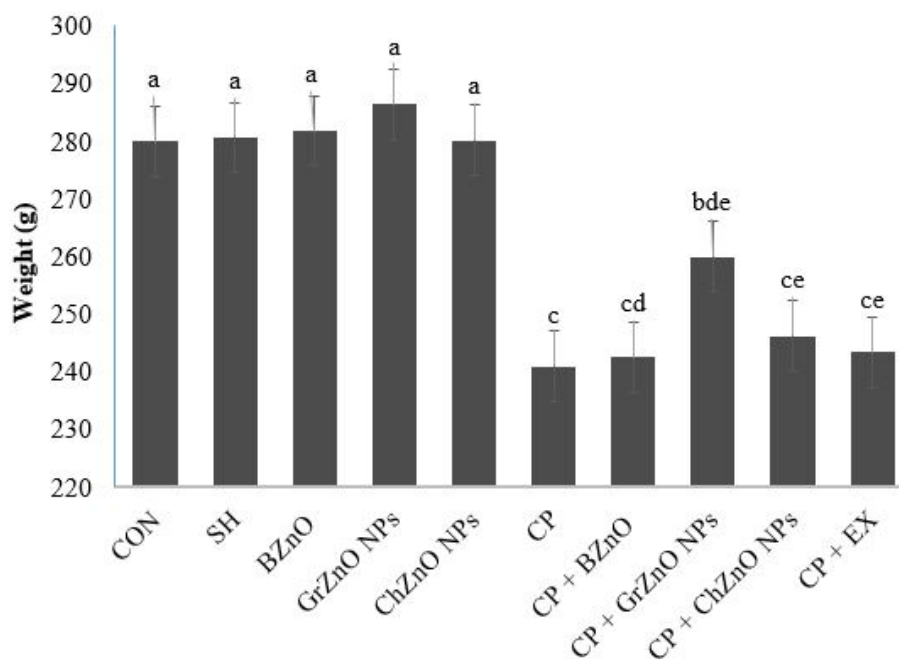

FIGURE 2 - Weight changes in different experimental groups. CON = Control group; SH = Sham group; BZnO = Bulk ZnO Group, (5 mg/kg daily for 4 weeks); GrZnO NPs = Green ZnO NPs Group, (5 mg/kg daily for 4 weeks); ChZnO NPs = Chemical ZnO NPs Group, (5 mg/kg daily for 4 weeks); CP = Cisplatin group, (5 mg/kg once a week for 4 weeks); CP + BZnO = Cisplatin + Bulk ZnO Group, (5 mg/kg CP once a week and 5 mg/kg BZnO NPs daily for 4 weeks); CP + GrZnO NPs = Cisplatin + Green ZnO NPs Group, (5 mg/kg CP once a week and 5 mg/kg GrZnO NPs daily for 4 weeks); CP + ChZnO NPs = Cisplatin + Chemical ZnO NPs Group, (5 mg/kg CP once a week and 5 mg/kg ChZnO NPs daily for 4 weeks); CP + EX = Cisplatin + Explant Group, (5 mg/kg CP once a week and 5 mg/kg *Aleo vera* extract daily for 4 weeks). Values are mean ± SD, n = 8 animals per group. Different letters in each column demonstrate significant difference (P < 0.05).

Serum BUN

The BUN level was significantly increased in the CP group compared to the control group (P <0.05). The BUN level in CP rats that treated by BZnO, GrZnO NPs and ChZnO NPs were significantly decreased compared to the untreated CP group (P <0.05). Administration of BZnO, GrZnO NPs and ChZnO NPs alone did not significantly change the BUN level compared to the control group (p < 0.05). (Table II).

Oxidative stress markers results

Antioxidant enzymes activities

Table II shows the changes of the SOD and CAT activities in the kidney of all experimental groups. The activities of CAT and SOD were significantly decreased in CP treated rats compared with the control group (P < 0.05). The antioxidant enzymes activities in CP-rats treated by BZnO, GrZnO NPs and ChZnO NPs were increased compared to the un treated CP group, but this change was only significant in the GrZnO NPs group compared to the groups that received ChZnO NPs or BZnO (P <0.05).

Administration of BZnO, GrZnO NPs and ChZnO NPs alone had no significant effects on the activities of antioxidant enzymes compared to the control group (p <0.05).

The lipid peroxidation levels

The MDA level, as lipid peroxidation indicators, in the kidney tissue was significantly higher after CP treatment compared with the control group ($P < 0.05$). The MDA level was significantly reduced in CP group that treated by BZnO, GrZnO NPs and ChZnO NPs compared to the untreated CP group (p<0.05). Administration of BZnO, GrZnO NPs and ChZnO NPs alone had no significant effect on MDA levels in control animals (Table II).

TABLE II - Oxidant/antioxidant markers of kidney serum and BUN level in different experimental groups

Group	CAT (U/mg protein)	SOD (U/mg protein)	MDA (nM/mg protein)	BUN (mg/dl)
CON	5.818 ± 0.33 [a]	2.809 ± 0.13 [a]	1.389 ± 0.24 [ac]	21.87 ± 2.42 [a]
SH	5.869 ± 0.32 [a]	2.351± 0.40 [a]	1.372 ± 0.10 [ac]	21.73 ± 2.71 [a]
BZnO	5.497 ± 0.17 [a]	2.409 ± 0.20 [a]	1.104 ± 0.13 [a]	21.48 ± 1.17 [a]
GrZnO NPs	5.522 ± 1.04 [a]	2.589 ± 0.38 [a]	1.151 ± 0.14 [a]	21.73 ± 2.24 [a]
ChZnO NPs	5.457 ± 1.29 [a]	2.558 ± 0.32 [a]	1.223 ± 0.21 [a]	21.74 ± 2.29 [a]
CP	2.393 ± 0.23 [b]	0.839 ± 0.08 [b]	4.483 ± 0.56 [d]	29.31 ± 0.74 [b]
CP + BZnO	2.675 ± 0.06 [b]	1.471 ± 0.25 [bc]	2.335 ± 0.32 [b]	22.43 ± 1.88 [a]
CP + GrZnO NPs	5.522 ± 0.32 [a]	2.138 ± 0.34 [ac]	2.517 ± 0.50 [b]	21.85 ± 2.03 [a]
CP + ChZnO NPs	3.421 ± 0.35 [b]	1.452 ± 0.25 [bc]	2.578 ± 0.28 [b]	22.47 ± 2.04 [a]
CP + EX	2.456 ± 0.17 [b]	1.081 ± 0.07 [b]	3.946 ± 0.68 [d]	22.49 ± 2.50 [a]

CON = Control group; SH = Sham group; BZnO = Bulk ZnO Group, (5 mg/kg daily for 4 weeks); GrZnO NPs = Green ZnO NPs Group, (5 mg/kg daily for 4 weeks); ChZnO NPs = Chemical ZnO NPs Group, (5 mg/kg daily for 4 weeks); CP = Cisplatin group, (5 mg/kg once a week for 4 weeks); CP + BZnO = Cisplatin + Bulk ZnO Group, (5 mg/kg CP once a week and 5 mg/kg BZnO NPs daily for 4 weeks); CP + GrZnO NPs = Cisplatin + Green ZnO NPs Group, (5 mg/kg CP once a week and 5 mg/kg GrZnO NPs daily for 4 weeks); CP + ChZnO NPs = Cisplatin + Chemical ZnO NPs Group, (5 mg/kg CP once a week and 5 mg/kg ChZnO NPs daily for 4 weeks); CP + EX = Cisplatin + Explant Group, (5 mg/kg CP once a week and 5 mg/kg *Aleo vera* extract daily for 4 weeks). Values are mean ± SD, n = 8 animals per group. Different letters in each column demonstrate significant difference ($P < 0.05$).

Expression of apoptosis related genes

The expression of *bax*, as an apoptotic gene, was significantly higher in the CP group compared to the control group (p < 0.05). The expression levels of the *bax* gene showed a significant reduction in the CP group that treated by BZnO, GrZnO NPs and ChZnO NPs compared to the CP group rats (P <0.05). This decrease was more significant in the GrZnO NPs group compared to groups that received other forms of ZnO (p < 0.05) (Figure 3A).

The expression of *bcl2*, as anti-apoptotic gene, was significantly decreased in the CP group compared to the control group (P <0.05). The expression levels of the *bcl2* gene was significantly increased in the CP group that treated by BZnO, GrZnO NPs and ChZnO NPs compared to the untreated CP group rats (P <0.05). This increase was more significant in the GrZnO NPs group compared to groups that received other forms of ZnO (p < 0.05) (Figure 3B).

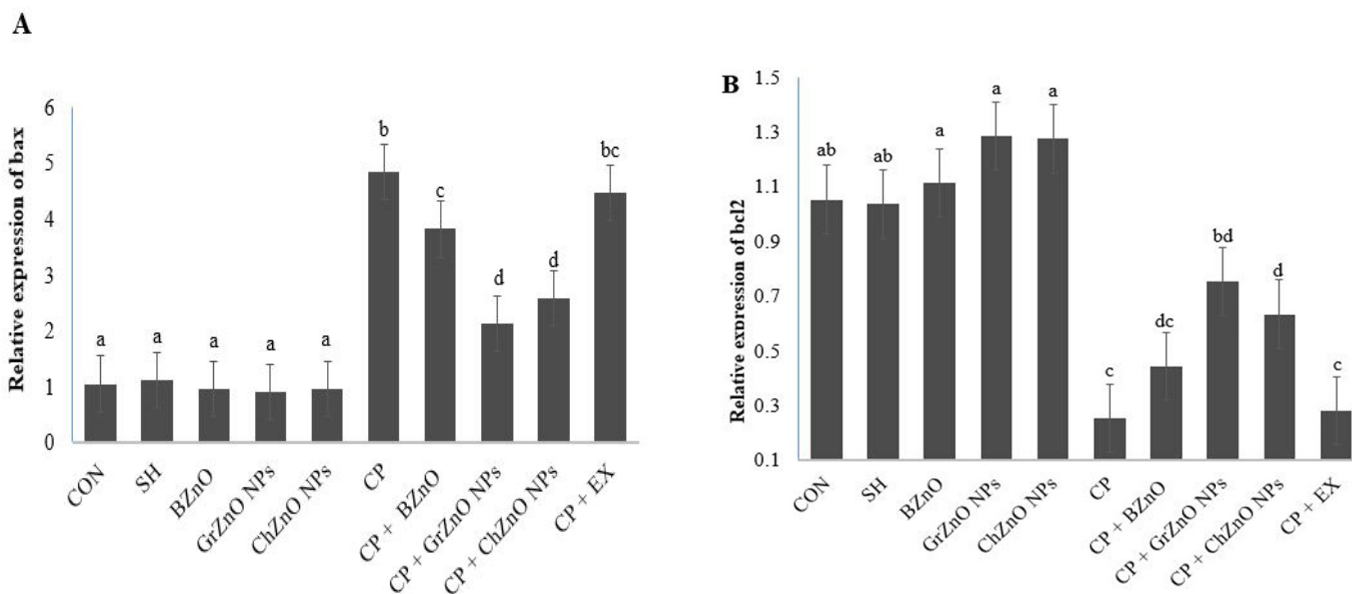**FIGURE 3** - Expression of apoptotic/antiapoptotoc genes (bax and bcl2) in the rat's kidney in different experimental groups. CON = Control group; SH = Sham group; BZnO = Bulk ZnO Group, (5 mg/kg daily for 4 weeks); GrZnO NPs = Green ZnO NPs Group, (5 mg/kg daily for 4 weeks); ChZnO NPs = Chemical ZnO NPs Group, (5 mg/kg daily for 4 weeks); CP = Cisplatin group, (5 mg/kg once a week for 4 weeks); CP + BZnO = Cisplatin + Bulk ZnO Group, (5 mg/kg CP once a week and 5 mg/kg BZnO NPs daily for 4 weeks); CP + GrZnO NPs = Cisplatin + Green ZnO NPs Group, (5 mg/kg CP once a week and 5 mg/kg GrZnO NPs daily for 4 weeks); CP + ChZnO NPs = Cisplatin + Chemical ZnO NPs Group, (5 mg/kg CP once a week and 5 mg/kg ChZnO NPs daily for 4 weeks); CP + EX = Cisplatin + Explant Group, (5 mg/kg CP once a week and 5 mg/kg *Aleo vera* extract daily for 4 weeks). Values are mean ± SD, n = 8 animals per group. Different letters in each column demonstrate significant difference (P < 0.05). Expression of apoptosis related genes was analyzed using qRT-PCR method and GAPDH was used as housekeeping gene.

Histological results

Microscopic observation showed a normal structure of the kidney with numerous healthy glomeruli and renal tubules (Figure 4A). The kidney showed remarkable microscopic changes in CP-treated groups. These notable changes were including the enlarged renal tubular epithelial. The sizes of these cells were 2-3 times bigger than the normal size. They had a large nucleus. Also, the shape of the nuclei was different and they showed pleomorphism. They had more than one nucleolus. Multinucleated cells (giant tumor cells) were seen in some renal tubules. Also, the tubular cells had clear cytoplasm with clear vacuoles. Necrosis of the cells lining renal tubules was observed (Figure 4B, C) and hyaline droplets were seen in some of them (Figure 4D). Multifocal non-purulent interstitial nephritis (Figure 4E) and hyaline casts (Figure 4F) were observed in some renal tubules. Renal pelvis mucosa cells showed necrosis in some areas and large amounts of erythrocytes were found

in the pelvis area (Figure 4G). Also, glomerulonephritis was observed. In some glomeruli, the capillary sheath occupied most of the capsule space (Figure 4H).

In the CP + BZnO groups, the observed changes were similar to those observed in the CP group. In this group, karyomegaly was observed along with vacuolation of cytoplasm lining cells renal tubular and necrosis (Figure 4I). Also, necrosis of the tubular cells was observed. In some areas, there was bleeding in the interstitial tissue. Erythrocytes were found in the pelvic space with the pelvic mucosa removed (Figure 4J).

A marked improvement was seen in the CP + GrZnO NPs. The changes in the nuclei of the tubular cells were decreased. Also, vacuolation in the cytoplasm, hyaline droplets, and hyaline casts were less than in other groups. Degeneration and necrosis of the tubular cells were less seen in the renal tubules. Erythrocytes with pink strands were also not seen in the pelvis (Figure 4K).

In the CP + ChZnO NPs group, the changes in the nuclei of the lining cells renal tubules were less observed.

Degeneration and necrosis of the cells lining were observed in the renal tubules. Hyaline droplets and hyaline casts were observed in the renal tubules. Erythrocytes with pink strands were also not seen in the pelvis (Figure 4L).
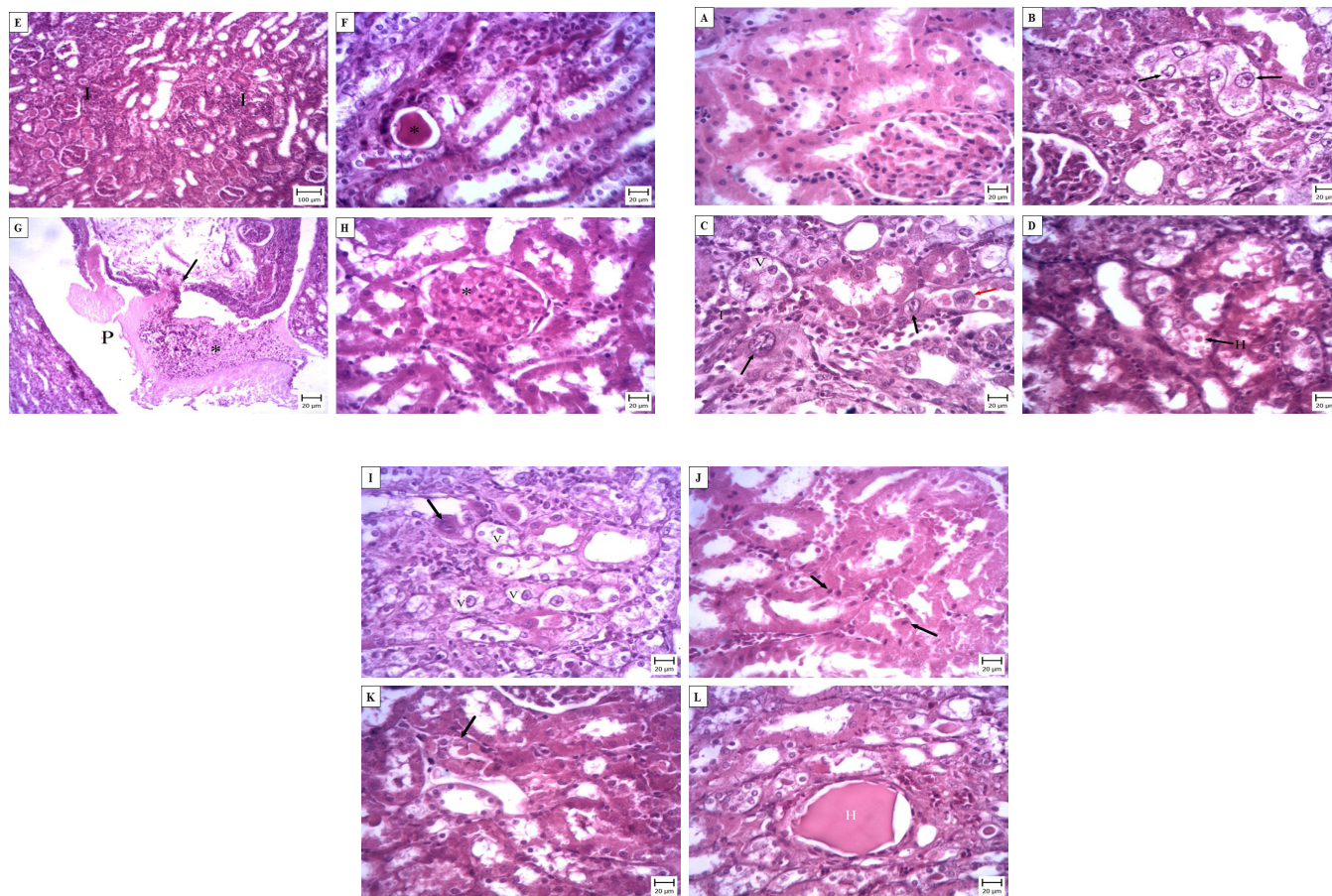

FIGURE 4 - Histological changes of kidney structure in different experimental groups, stained with H&E (A,B,C,D,F,G,H,I,J,K,L, bar: 20 μm; E, bar: 100 μm). (A): CON = Control group: Normal. (B,C,D,E,F,G,H): CP = Cisplatin group; Inculding (B): Cisplatin-induced caused degenerative changes incul the enlarged renal tubular epithelial (arrows). (C): cells had more than one nucleolus (red arrows), the tubular cells have clear cytoplasm with clear vacuoles (V), Multinucleated cells (giant tumor cells) (arrows), necrosis of the cells lining renal tubules (I). (D): Presence of hyaline droplet in some of cells (H). (E): Multi-focal non-purulent interstitial nephritis. (F): hyaline casts (star). (G): Renal pelvis mucosa cells showed necrosis in some areas (arrows) and large amounts of erythrocytes (star). (H): glomerulonephritis (star). (I): CP + BZnO (Cisplatin + Bulk ZnO Group), karyomegaly (arrows), vacuoles (V), necrosis (I). (J): Degeneration and necrosis of the cells lining renal tubules (arrows). (K): CP + GrZnO NPs (Cisplatin + Green ZnO NPs Group), GrZnO NPs administration improved degenerative changes induced by cisplatin. (L): CP + ChZnO NPs (Cisplatin + Chemical ZnO NPs Group), hyaline droplets and hyaline casts (H).

Administration of BZnO, GrZnO NPs and ChZnO NPs alone had no side effect on kidney histology compared with the control group.

According to a wide range of applications, CP has a wide range of negative effects such as accumulation of platinum in the kidney and impair its function (Barakat *et al*., 2020). Although mechanism of the CP is not yet specified, but it is well elucidated that nephrotoxicity of the CP is related to high generation of ROS (Zhang *et al*., 2019). The anticancer activity of cisplatin is dependent on its ability to bind to nuclear DNA and form complexes that are capable of preventing DNA synthesis and transcription (Ahmad, 2010). Also, cisplatin can bind mitochondrial DNA, that interferes with mitochondrial DNA transcription, and leads to reduced protein synthesis. A reduction in the expression of mitochondrial

DNA-encoded components of the electron transport chain disrupts respiration and consequently stimulate ROS production (Marullo *et al.*, 2013). So, it is possible that the increase in ROS production that occurs in the renal tubular cells, because the kidney can accumulate cisplatin at concentrations more than of other organs. The concentration of cisplatin in the epithelial cells of the proximal tubules can become 5 times more than that in the blood flow (Arany, Safirstein, 2003).

Increase in ROS production in kidney cells leads to in tubular cell death, that can cause cisplatin-induced nephrotoxicity. Cisplatin-induced nephrotoxicity usually starts a few days after cisplatin administration. ROS include the superoxide anion ($O2^-$), hydrogen peroxide ($H2O2$), and hydroxyl radicals ($OH·$) play important roles in the cisplatine induced nephrotoxicity. Although $O2^-$ is the precursor of $H2O2$, each species may play variable roles in cisplatin-induced nephrotoxicity, but $H2O2$ is more highly stable, can cross cell membranes, and can move farther to induce cell injury, while, $O2^-$ is more unstable, and can quickly transform into $H2O2$ by SOD enzyme (Quintanilha *et al.*, 2018).

The production of ROS, accumulation of lipid peroxidation products in kidneys, and disruption in the antioxidant systems are the main mechanisms of cisplatin-induced renal toxicity. Inside the cell, cisplatin is converted into a very reactive form fastly reacting with thiol-containing antioxidant molecules including glutathione. Thus, depletion of glutathione causes increased oxidative stress inside the cells (Barakat *et al.*, 2020). consequently, severe oxidative damage inside cells leads to tissue injury (Chan *et al.,* 2019). Previous studies reported that oxidative stress is the major mechanism responsible for cisplatin-induced nephrotoxicity (Quintanilha *et al.*, 2018). The oxidative stress leads to disturbance in the balance ROS production and decrease in the antioxidant defense mechanism (El-Shorbagy *et al.,* 2019).

Different antioxidant have been used to protect the kidneys against nephrotoxicity of CP. Antioxidants such as bismuth zinc (Chan *et al.,* 2019), zinc picolinate (Tuzcu *et al.*, 2010), zinc histidine (Srivastava *et al.*, 1995), and Zinc metallothionein (Salgueiro *et al.*, 2000), zinc sulfate (Joshi *et al.*, 2004), zinc gluconate (Huang *et al.*, 1997)

leads to decreased cisplatin-induced nephrotoxicity, inhibit cisplatin-induced apoptosis, improve the survival rate of mice treated with cisplatin and cause suppression the destructive effects of cisplatin on oxidative stress markers, without affecting its anticancer activity.

The emerging field of ZnO NPs possible create good motivation for against from CP-induced nephrotoxicity (Ashraf *et al.*, 2018). The present research was designed based on the usage of GrZnO NPs for possible amelioration of CP-induced nephrotoxicity in vivo. our results showed that the NPs at the defined dose and treatment schedule can restore the normal markers in CP-treated rats towards the control levels. The improvement effects of GrZnO NPs against different cancer cell lines have been reported in previous studies (Wilhelmi *et al.*, 2013; Siddiqui *et al.*, 2017). Previous studies have reported that the use of synthesized ZnO NPs by *P. caerulea L.* leaf extract can positively affect against urinary tract infections (Rajakumar *et al.*, 2018). Despite the fact that the biosynthesis of NPs is obscured by different plant extracts, it is indicated that the biomolecules present in the plant extract (protein, phenol and flavonoids) play an important role in reducing particle size and clogging of biosynthesized nanoparticles (Krishnaraj *et al.*, 2010).

In the present study, BUN level was increased in CP treated rats compared with the control groups, but it was decraesd in the GrZnO NPs. Also, the level of BUN was decreased in the CP groups treated with ZnO NPs, which it is in accordance with results of previous studies (Torabi, Shafaroudi, Rezaei, 2017; Ashraf *et al.*, 2018). CP can increase the levels of the kidney function biochemical marker such as BUN. These perturbations may be due to CP induced impairment of kidney reabsorption and increased reno-vascular resistance (Ashraf *et al.*, 2018). Also, CP exposure induces injury to the kidney vessels and finally causes glomerular filtration rate decline. This caused disruption of the kidney function and increase of the BUN levels (Torabi, Shafaroudi, Rezaei, 2017).

In the present study, CP treatment attenuated renal antioxidant defense but, the level of CAT and SOD activities were increased in the groups that received other forms of ZnO that this increased was more in the CP + GrZnO NPs group compared to other groups. The MDA concentration increased in the CP treated

group compared with the control group, indicating an induction of oxidative stress in the kidney of CP treated animals. The MDA concentration was decreased in the CP groups that treated by ZnO NPs which is in accordance with the results of previous studies (Torabi, Shafaroudi, Rezaei, 2017; Akca *et al*., 2018; Ashraf *et al*., 2018). Decrease in the activities of SOD with cisplatin treatment could be due to the direct connection of CP to _SH groups of functional cysteine residues, or probably via the oxidation of active site cysteine thiols groups by CP produced ROS. Cisplatin causes the removal of Cu and Zn that are important as cofactors for SOD activity and is probably another reason for the decreased SOD activity in the kidney tissues. CAT is an NADPH connecting protein and needs NADPH for biological activity. Decreased NADPH levels can also impair CAT activity (Ashraf *et al*., 2018). It is possible that the decrease in CAT activity, results in an increase in H_2O_2 after CP injection, which causes increased lipid peroxidation as a witness to significant changes in MDA levels in the cisplatin group (Norozi, Zare, 2012). previous studies have reported that Zn NPs enter the target cells and are separated and released slowly but continuously as Zn^{+2} ions. The antioxidant enzymes present in such cells can easily detect these ions. Ions can enhance the activity of essential antioxidant enzymes in treated cells (Bashandy *et al*., 2018). In similar studies, GrZnO NPs have had the same effect on oxidative stress indices and antioxidant enzymes (Alkaladi, Abdelazim, Afifi, 2014; Al-Salmi, Hamza, El-Shenawy, 2019). It was reported that ZnO NPs/ Green Tea Extract (ZnO NPs/GTE) in rats treated with monosodium glutamate is associated with significant improvement in all antioxidant parameters such as SOD, CAT and MDA that were modified by monosodium glutamate (Hamza, Al-Salmi, El-Shenawy, 2019). ZnO NPs improve the oxidative stress in diabetic rats via an increase in the activities of mRNA expression levels of SOD, CAT and a decrease in MDA concentration (Afifi, Abdelazim, 2015).

The ZnO-NPs cross quickly via cell membrane and connect with cellular macromolecules leading to therapeutic effect on some organs. Food and Drug Organization approved ZnO-NPs as anticancer drug (Barakat *et al*., 2020). The isoelectric point of ZnO-NPs equals 9–10; So, ZnO-NPs will have a high positive surface charge in tissue fluid. Cancer cells have a greater concentration of negatively phospholipids on their outer membrane. Consequently, an electrostatic attraction occurs among ZnO-NPs and cancer cells cause a higher level of Zn in the tumor tissue compared to the other healthy tissues (El-Shorbagy *et al.,* 2019).

Our results showed that, the expression of *bax* gene was increased and the expression of *bcl2* gene was decreased in kidney of CP-treated rats compared with the control group. Several previous studies have reported similar findings in CP treatment experimental animals (Tsuruya *et al*., 2003; Zhou *et al*., 2003). CP induces the process of apoptosis via starting the cytochrome c emission and resulting in the production of superoxide (Yousef, Hussien, 2015). Tubular cell apoptosis is one of the main mechanisms that causes CP-induced renal damage (Li *et al*., 2015). In our study, ZnO NPs could prevent CP-induced tubular cells apoptosis in renal tubular cells. Zinc may participate in the inhibition of apoptosis by stabilizing the biomembranes, also indirectly as an antioxidant (Prasad, 2004). Tian *et al*. (2009) reported that one of the ZnO NPs properties is its anti-apoptotic properties. Zinc deficiency can cause programmed cell death in different cell types, while zinc supplementation can protect cells against various propoptosis molecules, and prevent apoptosis. It has been proved that one of the possible mechanisms of reducing apoptosis is inhibition of caspase enzyme activity which regulates *bax*, and *bcl2* expression. Another possibility of obtained results is that ZnO NPs may increase mitochondrial function to decrease the release of apoptosis inducing factor and cytochrome c that causes apoptosis in cells as an internal signals, eventually prevent cell apoptosis (Tian *et al*., 2009). The co-treatment of BiZn effectively prevents cisplatin-induced apoptosis of renal cells. The BiZn treatment could significantly improve the survival rate with lethal dose of cisplatin. Thus, with the help of BiZn, more doses of cisplatin can be used for patients with refractory tumors or organ toxicity. They found that BiZn did not affect cisplatin-induced cytotoxicity on neuroblastoma cells under both in vitro and in vivo models. (Chan *et al.,* 2019).

The results of histology (Figure 3) showed obvious tissue injuries in the kidney of CP treated animals such as vacuolization, severe necrosis, hyaline droplets formation, multi-focal, degenerative changes in cells lining renal tubules and desquamation of degenerated cells present in the lumen of the tubules which is in accordance with the results of previous studies (Yao *et al.*, 2007; Yousef, Hussien, 2015; Ashraf *et al.*, 2018). Histopathological reviews of CP-induced renal tissue shows induction of apoptosis by CP produced free radicals (Zhang *et al.*, 2019). In accordance with previous studies (Yousef, Hussien, 2015; Bashandy *et al.*, 2018; El-Shenawy *et al.*, 2019), in the rats treated with ZnO NPs concomitant with CP, a marked improvement in renal histological abnormalities was observed but with mild degeneration of the renal epithelial tubular and glomeruli, with focal areas of less extensive glomerular necrosis. Previous research has found that ZnO NPs can enhance the reparation of epithelial cells (Dawei, Zhisheng, Anguo, 2010). ZnO NPs with the free radical scavenging activity, caused the decrease of lipid peroxidation and enhancement of antioxidant enzymes (CAT and SOD) that improves the renal kidney injury and decrease the pathological changes in CP group rats treated with ZnO NPs (Yousef, Hussien, 2015; Bashandy *et al.*, 2018). These results are consistent with Zheng et al. and Reham et al. who confirmed that GrZnO NPs do not have any toxic effects on the kidney tissues (Wang *et al.*, 2008; Hamza, Al-Salmi, El-Shenawy, 2019).

CONCLUSION

The results suggest that administration of three forms of ZnO NPs (BZnO, ChZnO NPs, and GrZnO NP) and especially GrZnO NPs during CP chemotherapy can effectively reduce the oxidative stress of its nephrotxcity and kidney structure damage. Thus, GrZnO NPs may be an attractive treatment during CP chemotherapy that could provide a better quality of life for cancer patients.

ACKNOWLEDGEMENTS

REFERENCES

Afifi M, Abdelazim AM. Ameliorative effect of zinc oxide and silver nanoparticles on antioxidant system in the brain of diabetic rats. Asian Pac J Trop Biomed. 2015;5(10):874-877.

Ahmad S. Platinum–DNA interactions and subsequent cellular processes controlling sensitivity to anticancer platinum complexes. Chem Biodivers. 2010;7(3):543-566.

Akca G, Eren H, Tumkaya L, Mercantepe T, Horsanali MO, Deveci E, et al. The protective effect of astaxanthin against cisplatin-induced nephrotoxicity in rats. Biomed Pharmacother. 2018;100:575-582.

Alkaladi A, Abdelazim AM, Afifi M. Antidiabetic activity of zinc oxide and silver nanoparticles on streptozotocin-induced diabetic rats. Int J Mol Sci. 2014;15(2):2015-2023.

Al-Salmi FA, Hamza RZ, El-Shenawy NS. The Interaction of Zinc Oxide/Green Tea Extract complex nanoparticles and its effect on monosodium glutamate toxicity in liver of rats. Curr Pharm Biotechnol. 2019;20(6):465-475.

Arany I. Safirstein RL. Cisplatin nephrotoxicity. Semin Nephrol. 2003;23:460-464.

Ashraf JM, Ansari MA, Fatma S, Abdullah SM, Iqbal J, Madkhali A, et al. Inhibiting effect of zinc oxide nanoparticles on advanced glycation products and oxidative modifications: A potential tool to counteract oxidative stress in neurodegenerative diseases. Mol Neurobiol. 2018;55(9):7438-7452.

Barakat LA, Barakat N, Zakaria MM, Khirallah SM. Protective role of zinc oxide nanoparticles in kidney injury induced by cisplatin in rats. Life Sci. 2020;262:118503.

Bashandy SA, Alaamer A, Moussa SAA, Omara EA. Role of zinc oxide nanoparticles in alleviating hepatic fibrosis and nephrotoxicity induced by thioacetamide in rats. Can J Physiol Pharmacol. 2018;96(4):337-344.

Chan S, Wang R, Man K, Nicholls J, Li H, Sun H, Chan GC. A novel synthetic compound, bismuth zinc citrate, could potentially reduce cisplatin-induced toxicity without compromising the anticancer effect through enhanced expression of antioxidant protein. Transl Oncol. 2019;12(5):788-799.

Dawei AI, Zhisheng W, Anguo Z. Protective effects of Nano-ZnO on the primary culture mice intestinal epithelial cells in in vitro against oxidative injury. World J Agr Sci. 2010;6(2):149-153.

El-Shenawy NS, Hamza RZ, Al-Salmi FA, Al-Eisa RA. Evaluation of the effect of nanoparticles zinc oxide/ camellia sinensis complex on the kidney of rats treated

with monosodium glutamate: antioxidant and histological approaches. Curr Pharm Biotechnol. 2019;20(7):542-550.

El-Shorbagy HM, Eissa SM, Sabet S, El-Ghor AA. Apoptosis and oxidative stress as relevant mechanisms of antitumor activity and genotoxicity of ZnO-NPs alone and in combination with N-acetyl cysteine in tumor-bearing mice. Int J Nanomed. 2019;14:3911.

Hamza RZ, Al-Salmi FA, El-Shenawy NS. Evaluation of the effects of the green nanoparticles zinc oxide on monosodium glutamate-induced toxicity in the brain of rats. PeerJ. 2019;7:e7460.

Huang Y, Zhou S, Qui L, Wu J, Xu C. Effects of zinc gluconate on nephrotoxicity and glutathione metabolism disorder induced by cis-platin in mice. Drug Metab Drug Interact. 1997;14(1):41-46.

Iravani S. Green synthesis of metal nanoparticles using plants. Green Chem. 2011;13(10):2638-2650.

Jeevanandam J, Chan YS, Danquah MK. Biosynthesis of metal and metal oxide nanoparticles. ChemBioEng Rev. 2016;3(2):55-67.

Joshi SE, Hasan SK, Chandra R, Husain MM, Srivastava RC. Scavenging action of zinc and green tea polyphenol on cisplatin and nickel induced nitric oxide generation and lipid peroxidation in rats. Biomed Environ Sci. 2004;17(4):402-409.

Khan SA, Noreen F, Kanwal S, Iqbal A, Hussain G. Green synthesis of ZnO and Cu-doped ZnO nanoparticles from leaf extracts of Abutilon indicum, Clerodendrum infortunatum, Clerodendrum inerme and investigation of their biological and photocatalytic activities. Mater Sci Eng C. 2018;82:46-59.

Kiyani MM, Butt MA, Rehman H, Ali H, Hussain SA, Obaid S, et al. Antioxidant and anti-gout effects of orally administered zinc oxide nanoparticles in gouty mice. J Trace Elem Med Biol. 2019;56:169-177.

Koroliuk MA, Ivanova MI, Mayorova IG. Tokarev VE. The method for determining the activity of catalase [in Russian]. Lab Delo. 1988;1:16-9.

Krishnaraj C, Jagan E, Rajasekar S, Selvakumar P, Kalaichelvan P, Mohan N. Synthesis of silver nanoparticles using Acalypha indica leaf extracts and its antibacterial activity against water borne pathogens. Colloids Surf B Biointerfaces. 2010;76(1):50-56.

Kröning R, Lichtenstein AK, Nagami GT. Sulfur-containing amino acids decrease cisplatin cytotoxicity and uptake in renal tubule epithelial cell lines. Cancer Chemother Pharmacol. 2000;45(1):43-49.

Li S, Tan HY, Wang N, Zhang ZJ, Lao L, Wong CW, et al. The role of oxidative stress and antioxidants in liver diseases. Int J Mol Sci. 2015;16(11):26087-26124.

Marullo R, Werner E, Degtyareva N, Moore B, Altavilla G, Ramalingam SS, Doetsch PW. Cisplatin induces a mitochondrial-ROS response that contributes to cytotoxicity depending on mitochondrial redox status and bioenergetic functions. PloS one. 2013;8(11):e81162.

Norozi M, Zare S. Evaluation of the effects of taurine on cisplatin-induced kidney injury and oxidative stress in male rats. J Physiol Pharmacol. 2012;15(4):478-485.

Pabla N, Dong Z. Cisplatin nephrotoxicity: mechanisms and renoprotective strategies. Kidney Int. 2008;73(9):994-1007.

Prasad AS, Bao B, Beck FW, Kucuk O, Sarkar FH. Antioxidant effect of zinc in humans. Free Radic Biol Med. 2004;37(8):1182-1190.

Quintanilha JC, Visacri MB, Sousa VM, Bastos LB, Vaz CO, Guarnieri JP, Amaral LS, Malaguti C, Lima CS, Vercesi AE, Moriel P. Cisplatin-induced human peripheral blood mononuclear cells' oxidative stress and nephrotoxicity in head and neck cancer patients: the influence of hydrogen peroxide. Mol Cell Biochem. 2018;440(1-2):139-145.

Rabeea IS, Al Dujeli AAB, Rizij FAJ, Hussein AA. Effect of zinc sulfate on kidney function in cisplatin-treated cancer patients. Karbala J Med. 2016;9(2):2505-2512.

Rajakumar G, Thiruvengadam M, Mydhili G, Gomathi T, Chung I-M. Green approach for synthesis of zinc oxide nanoparticles from Andrographis paniculata leaf extract and evaluation of their antioxidant, anti-diabetic, and anti-inflammatory activities. Bioprocess Biosyst Eng. 2018;41(1):21-30.

Roy B, Baghel RPS, Mohanty TK, Mondal G. Zinc and male reproduction in domestic animals: A review. Indian J Anim Nutr. 2013;30(4):339-350.

Salgueiro MJ, Zubillaga M, Lysionek A, Sarabia MI, Caro R, De Paoli T, Hager A, Weill R, Boccio J. Zinc as an essential micronutrient. Nutr Res Rev. 2000;20(5):737-755.

Santhoshkumar J, Kumar SV, Rajeshkumar S. Synthesis of zinc oxide nanoparticles using plant leaf extract against urinary tract infection pathogen. Resour-Effic Technol. 2017;3(4):459-465.

Satoh K. Serum lipid peroxide in cerebrovascular disorders determined by a new colorimetric method. Clinica chimica acta. 1978;15:37-43.

Sharmila G, Thirumarimurugan M, Muthukumaran C. Green synthesis of ZnO nanoparticles using Tecoma castanifolia leaf extract: characterization and evaluation of its antioxidant, bactericidal and anticancer activities. Microchem J. 2019;145:578-587.

Siddiqui MA, Wahab R, Ahmad J, Farshori NN, Saquib Q, Khan ST, et al. Zinc oxide nanoparticles: mechanism (s) of

cell death induced in human epidermoid larynx cell line (HEp-2). Nanosci Nanotechnol Lett. 2017;9(4):573-582.

Srivastava RC, Farookh A, Ahmad N, Misra M, Hasan SK, Husain MM. Reduction of cis-platinum induced nephrotoxicity by zinc histidine complex: the possible implication of nitric oxide. Biochem Mol Biol Int. 1995;36(4):855-862.

Tian L, Zhu F, Ren H, Jiang J, Li W. Effects of nano-zinc oxide on antioxidant function in broilers. Chinese J Anim Nutr. 2009;21(4):534-539.

Torabi F, Shafaroudi MM, Rezaei N. Combined protective effect of zinc oxide nanoparticles and melatonin on cyclophosphamide-induced toxicity in testicular histology and sperm parameters in adult Wistar rats. Int J Reprod Biomed. 2017;15(7):403.

Torabi M, Kesmati M, Harooni HE, Varzi HN. Different efficacy of nanoparticle and conventional ZnO in an animal model of anxiety. Neurophysiol. 2013;45(4):299-305.

Tsuruya K, Ninomiya T, Tokumoto M, Hirakawa M, Masutani K, Taniguchi M, et al. Direct involvement of the receptor-mediated apoptotic pathways in cisplatin-induced renal tubular cell death. Kidney Int. 2003;63(1):72-82.

Tuzcu M, Sahin N, Dogukan A, Aslan A, Gencoglu H, Ilhan N, Kucuk O, Sahin K. Protective role of zinc picolinate on cisplatin-induced nephrotoxicity in rats. J Renal Nutr. 2010;20(6):398-407.

Wang B, Feng W, Wang M, Wang T, Gu Y, Zhu M, et al. Acute toxicological impact of nano-and submicro-scaled zinc oxide powder on healthy adult mice. J Nanopart Res. 2008;10(2):263-276.

Wilhelmi V, Fischer U, Weighardt H, Schulze-Osthoff K, Nickel C, Stahlmecke B, et al. Zinc oxide nanoparticles induce necrosis and apoptosis in macrophages in a p47phox- and Nrf2-independent manner. PloS One. 2013;8(6):e65704.

Yao X, Panichpisal K, Kurtzman N, Nugent K. Cisplatin nephrotoxicity: a review. Am J Med Sci. 2007;334(2):115-124.

Yousef MI, Hussien HM. Cisplatin-induced renal toxicity via tumor necrosis factor-α, interleukin 6, tumor suppressor P53, DNA damage, xanthine oxidase, histological changes, oxidative stress and nitric oxide in rats: protective effect of ginseng. Food Chem Toxicol. 2015;78:17-25.

Zhang Z, Xin G, Zhou G, Li Q, Veeraraghavan VP, Krishna Mohan S, et al. Green synthesis of silver nanoparticles from Alpinia officinarum mitigates cisplatin-induced nephrotoxicity via down-regulating apoptotic pathway in rats. Artif Cells Nanomed Biotechnol. 2019;47(1):3212-3221.

Zhou H, Kato A, Yasuda H, Odamaki M, Itoh H, Hishida A. The induction of heat shock protein-72 attenuates cisplatin-induced acute renal failure in rats. Pflügers Archiv. 2003;446(1):116-124.